

# Clustering at 74 MHz

Angélica de Oliveira-Costa & John Capodilupo

MIT Kavli Institute & Dept. of Physics, Massachusetts Institute of Technology, Cambridge, MA 02139

(Dated: November 1, 2018. To be submitted to MNRAS.)

In order to construct accurate point sources simulations at the frequencies relevant to 21 cm experiments, the angular correlation of radio sources must be taken into account. Using the 74 MHz VLSS survey, we measured the angular 2-point correlation function,  $w(\theta)$ . We obtain the first measurement of clustering at the low frequencies relevant to 21 cm tomography. We find that a single power law with shape  $w(\theta) = A\theta^{-\gamma}$  fits well the data. For a galactic cut of  $|b| > 10$ , with a data cut of  $\delta > -10$ , and a flux limit of  $S = 770$  mJy, we obtain a slope of  $\gamma = (-1.2 \pm 0.35)$ . This value of  $\gamma$  is consistent with that measured from other radio catalogues at the millimeter wavelengths. The amplitude of clustering has a length of 0.2–0.6, and it is independent of the flux-density threshold.

## I. INTRODUCTION

Progress in detector, space and computer technology has triggered an avalanche of high-quality cosmological data, removing cosmology from the realm of philosophy and transforming it into a quantitative empirical science. In the past few years, many authors have argued that the 21cm tomography, *i.e.*, the three-dimensional mapping of highly redshifted 21cm emission, will be the ultimate cosmological probe – see, *e.g.*, [1, 2, 3, 4, 5, 6, 7, 8, 9, 10, 11]. Although this signal has yet to be detected, there is a theoretical consensus that the 21 cm signal must be out there and would be extremely useful if measured. [12, 13, 14, 15, 16, 17]

Although ambitious experimental efforts in 21cm tomography are now in progress across the globe (see Table I), it is widely known/understood that the cosmological results of these experiments will only be as good as our ability to deal with (or to remove) foreground contamination [18, 19, 20, 21, 22, 23, 24]. The goal of this work is to support these worldwide experimental efforts by tackling the foreground issue.

Understanding the physical origin of Galactic metre wavelength emission is interesting for two reasons: to determine the fundamental properties of the Galactic components, and to refine the modeling of foreground emission for cosmological 21 cm experiments. At metre wavelengths, the bulk of foreground contamination is due to synchrotron emission. When coming from extragalactic objects, this radiation is usually referred to as point source contamination and affects mainly small angular scales. When coming from the Milky Way, this diffuse Galactic emission fluctuates mainly on large angular scales [21].

Normal galaxies, radio galaxies and active galactic nuclei form the majority of extragalactic continuum sources [25]. A number of surveys of radio sources have been performed at frequencies relevant to the 21 cm tomography – see Table II; and analysis of these catalogs have helped to bring some understanding about their statistical properties: the distribution of radio sources is found to obey Poisson statistics with very weak observed angular clustering – see Table III.

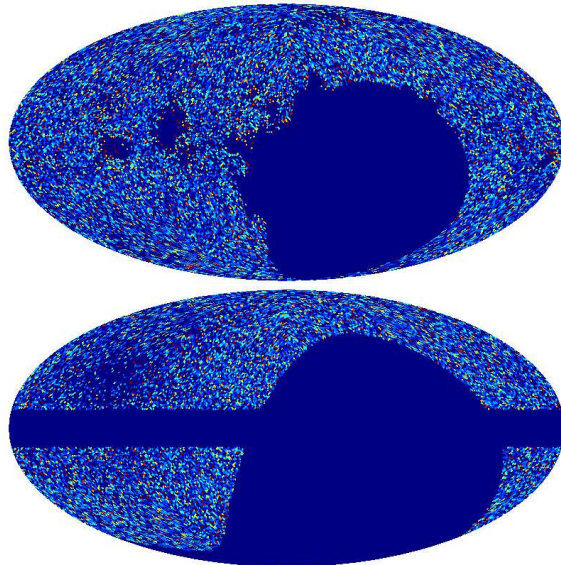


FIG. 1: The 74 MHz VLSS catalogue (top), and one of our 74 MHz mock catalogues (bottom). Both catalogues are plotted in the interval of  $(0 \leq S \leq 5)$  Jy, and in Galactic coordinates with the Galactic center at the origin and longitude increasing to the left. The mock catalogue also shows the final area used in our analysis ( $\delta \geq -10$  and  $|b| \geq 10$ ).

Some aspects of both experimental design optimization and actual data analysis require full-blown simulations of the sky signal and knowledge about how it propagates through the instrument and the data analysis pipeline — this has motivated the ambitious simulation efforts carried out by, *e.g.*, WMAP and Planck. End-to-end simulations are at least as important for 21 cm experiments because of the many complicated issues related to instrumental performance, ionospheric turbulence corrections, *etc.* [19, 26, 27, 28, 29]. In order to construct accurate simulations at the metre wavelengths, the angular correlation of radio sources must be taken into account [30]. It is important to point out that the relative importance of the clustering contribution increases and may eventually become dominant if sources are identified and subtracted down to faint flux limits [28] – which are exactly the limits involved in the point source removal of 21 cm experiments.

TABLE I: 21 cm Tomography Experiments.

Experiment	FWHM	$\nu$ [MHz]	Receiver	Sensitivity	Effective Area [m <sup>2</sup> ]	Site-yr
GMRT	3.8-0.4	50-1420	30 dishes	15 mK/ $\sqrt{day}$	5.10 <sup>4</sup>	India - 2007
PAST/21CMA	3'	50-200	10,000 antennas		7.10 <sup>4</sup>	Ulaistai,CH - 2007
LOFAR	25"-3.5"	10-240	25,000 dipole antennas		1.10 <sup>5</sup>	Drenthe,NL - 2007
MWA	15'	80-300	8,192 dipole antennas		1.10 <sup>4</sup>	Murchison,AU - 2007
PAPER		110-200	16 antennas		1.10 <sup>4</sup>	USA/AU - 2008
SKA	0.1"	100-25GHz				AU(?) - 2015(?)

GMRT = Giant Metrewave Radio Telescope, see <http://www.gmrt.ncra.tifr.res.in/>.

PaST/21CMA = Primeval Structure Telescope, see <http://web.phys.cmu.edu/~past/>.

LOFAR = LOw Frequency ARray, see <http://www.lofar.org>.

MWA = Murchison Widefield Array, see <http://www.haystack.mit.edu/ast/arrays/mwa/index.html>.

PAPER = Precision Array to Probe Epoch of Reionization, see <http://astro.berkeley.edu/~dbacker/eor/>.

SKA = Square Kilometer Array, see <http://www.skatelescope.org>.

TABLE II: Publicly available point source catalogues at the frequencies relevant to 21-cm tomography.

Ref	$\nu$ [MHz]	Region	FWHM [arcmin]	$S_{comp}$ [Jy]	$S_{min}$ [Jy]	$N_{obj}$	Observatory	Status
[31]	38	00 <sup>h</sup> < $\alpha$ <24 <sup>h</sup> +60< $\delta$ <+90.	4.5	0.77	1	5859	CLFST, ENG	A
[32]	60	00 <sup>h</sup> < $\alpha$ <24 <sup>h</sup> +55< $\delta$ <+55.	450		12	100	Pushchino, RUS	B
[58]	74	00 <sup>h</sup> < $\alpha$ <24 <sup>h</sup> -30< $\delta$ <+90.	1.33		68311		VLA, USA	A
[33]	80	00 <sup>h</sup> < $\alpha$ <24 <sup>h</sup> -49< $\delta$ <+37.	3.7		2	999	Culgoora, ENG	A
[33]	80	00 <sup>h</sup> < $\alpha$ <24 <sup>h</sup> -49< $\delta$ <+37.	3.7		2	1748	Culgoora, ENG	A
[34]	81	00 <sup>h</sup> < $\alpha$ <24 <sup>h</sup> +70< $\delta$ <+90.	10		1	558	Cambridge, ENG	B
[35]	102	00 <sup>h</sup> < $\alpha$ <24 <sup>h</sup> +27< $\delta$ <+70.	60	2	3	920	LPA, RUS	A
[36]	150	18 <sup>h</sup> < $\alpha$ <24 <sup>h</sup> -70< $\delta$ <-10.	4.6		0.96	2784	MRT, India	A
[37]	151	00 <sup>h</sup> < $\alpha$ <24 <sup>h</sup> +30< $\delta$ <+90.	4.2		0.13	34418	CLFST, ENG	A
[38]	151	00 <sup>h</sup> < $\alpha$ <24 <sup>h</sup> +21< $\delta$ <+90.	1.2		0.120	43689	CLFST, ENG	A
[39]	159	00 <sup>h</sup> < $\alpha$ <24 <sup>h</sup> -22< $\delta$ <+71.	10.0		7	471	Cambridge, ENG	A
[33]	160	00 <sup>h</sup> < $\alpha$ <24 <sup>h</sup> -49< $\delta$ <+37.	1.85		1.2	2041	Culgoora, ENG	A
[40]	178	00 <sup>h</sup> < $\alpha$ <24 <sup>h</sup> -90< $\delta$ <-05.	6.0	2	5	11000	Cambridge, ENG	A
[41, 42]	178	00 <sup>h</sup> < $\alpha$ <24 <sup>h</sup> -07< $\delta$ <+80.	11.5		2	4844	4C Array, ENG	A
[43]	232	00 <sup>h</sup> < $\alpha$ <24 <sup>h</sup> +30< $\delta$ <+90.	3.8		0.1	34426	MSRT, CHI	A
[44]	325	00 <sup>h</sup> < $\alpha$ <24 <sup>h</sup> +30< $\delta$ <+90.	0.9		0.1	229420	WSRT, NLD	A
[45]	352	00 <sup>h</sup> < $\alpha$ <24 <sup>h</sup> -09< $\delta$ <+26.	0.9		0.010	84481	WSRT, NLD	A
[46]	365	00 <sup>h</sup> < $\alpha$ <24 <sup>h</sup> +36< $\delta$ <+72.	0.1		0.25	66841	UTRAO, USA	A

$S_{comp}$  = Limit of completeness.

$S_{min}$  = Smallest flux value.

$N_{obj}$  = Number of sources in the catalogue.

A = Publicly available in digital form.

B = Available as printed table (which we will OCR).

TABLE III: Published  $w(\theta)^1$  values.

Ref	$\nu$ [GHz]	A $\times 10^{-3}$	$\gamma$	$w(\theta)$ □	$S_{lim}$ [mJy]
[47]	0.178			1.50–3.0	3000
[48]	0.325	$1.0 \pm 0.4$	$1.22 \pm 0.33$	$> 0.2$	35
[49]	0.408			–	250
[50]	0.408			–	10
[48]	0.843	$2.0 \pm 0.4$	$1.24 \pm 0.16$	$> 0.2$	10
[51]	1.400	$2.6 \pm 0.8$	$1.2 \pm 0.1$	0.07–4.0	3
[52]	1.400	$1.1 \pm 0.1$	$1.5 \pm 0.1$	$> 0.07$	3
[53]	1.400	$1.0 \pm 0.3$	$0.9 \pm 0.2$	$> 0.07$	3
[53, 54]	1.400	$1.0 \pm 0.2$	$0.7 \pm 0.1$	$> 0.1$	10
[48]	1.400	$1.5 \pm 0.2$	$1.05 \pm 0.10$	$> 0.3$	10
[49]	2.7			–	350
[55]	4.850			0.70–1.7	45
[56]	4.850		0.8	0.30–1.9	35
[57]	4.850	$10.0 \pm 5.0$	0.8	0.01–1.0	50

<sup>1</sup> $w(\theta)$  is fitted by a power-law of the form  $A\theta^{-\gamma}$   
 $S_{lim}$  = Smallest flux value.

In this paper, we present measurements of the angular 2-point correlation function,  $w(\theta)$ , from the 74 MHz VLSS survey [58]. We obtain the first measurement of clustering at the low frequencies relevant to 21 cm tomography. In Section II, we described the statistical tools used in this analysis, as well as the 74 MHz VLSS survey. In Section III, we describe our results, and in Section IV, we present our conclusions.

## II. DATA ANALYSIS TOOLS

### A. The Angular 2-point Correlation Function

In recent years, the analysis of the correlation-function has become the standard way of quantifying the clustering of different populations of astronomical sources. Specifically, the angular two-point correlation function  $w(\theta)$  gives the excess probability  $\delta P$ , in comparison to a random Poisson distribution, of finding two sources in a solid angle  $\delta\Omega_1$  and  $\delta\Omega_2$  separated by the angle  $\theta$ .  $\delta P$  is defined as

$$\delta P = N^2 \delta\Omega_1 \delta\Omega_2 [1 + w(\theta)], \quad (1)$$

where  $N$  is the mean number density of objects in the catalogue under consideration [59].

Many derivations for estimators of  $w(\theta)$  can be found in the literature (see, *e.g.*, [59, 60, 61]). One way to estimate this function is to compare the distribution of the objects in the real catalogue to the distribution of points in a random Poisson distributed catalogue with

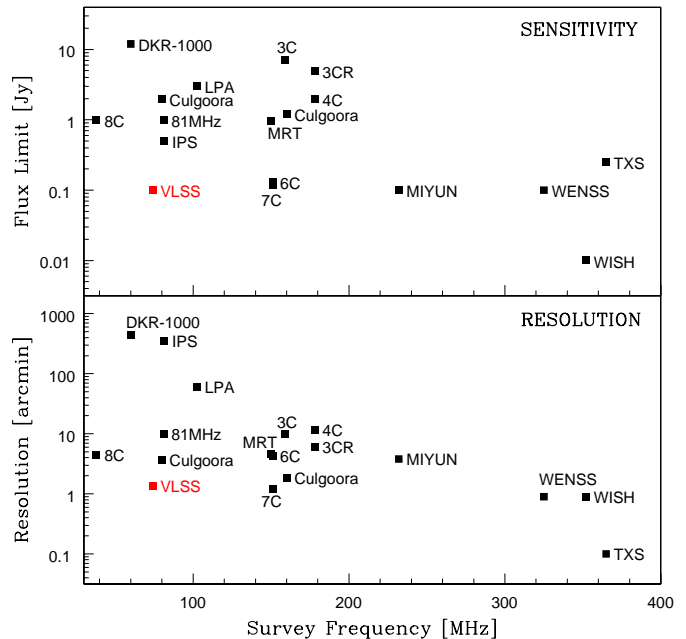


FIG. 2: A comparison between point source sensitivity and resolution of the 74 MHz VLSS survey (in red) and other low frequency surveys (see Table II).

the same boundaries, or

$$w(\theta) = \frac{DD(\theta) * RR(\theta)}{[DR(\theta)]^2} - 1 \quad (2)$$

[61], where  $DD(\theta)$ ,  $RR(\theta)$  and  $DR(\theta)$  are the numbers of data-data, random-random and data-random pairs separated by the distance  $\theta + \delta\theta$ . It is important to remember that the estimation of  $RR(\theta)$  and  $DR(\theta)$  requires a catalogue of objects scattered uniformly over an area with the same angular boundaries of the data catalogue.

### B. Mock Catalogues

We used the ‘‘Sphere Point Picking Algorithm’’ [62] to generate random cartesian vectors equally distributed on the surface of a unit sphere (to avoid having vectors ‘‘bunched’’ around the poles, as it would happen if one chooses to plot the vectors in spherical coordinates instead). Accordingly, we calculate these vectors by doing

$$x = \sqrt{1 - u^2} \cos \theta \quad (3)$$

$$y = \sqrt{1 - u^2} \sin \theta \quad (4)$$

$$z = u, \quad (5)$$

where  $u = \cos \phi$ , with  $\theta \in [0, 2\pi)$  and  $u \in [-1, 1]$  [63]. In order to obtain points such that any small area on the sphere is expected to contain the same number of points, we choose  $u$  and  $v$  to be random variates in the interval

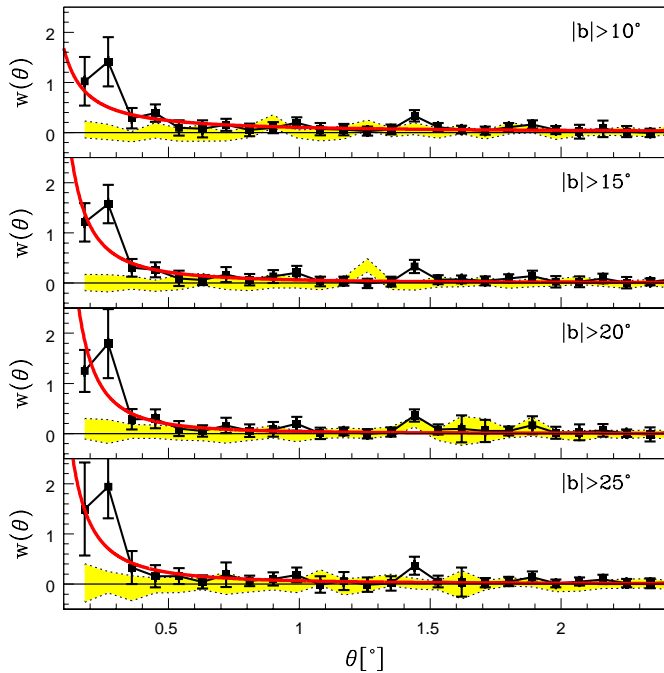


FIG. 3: Measured  $w(\theta)$  for different galactic cuts. All angular correlations are calculated at the flux limit of  $S = 770$  mJy. The red lines are single power law fits to the data, where  $w(\theta) = A\theta^{-\gamma}$ ; and the yellow shaded regions are  $w(\theta)$  calculated using solely mocks.

$[0, 1]$ . Therefore, we calculate  $\theta$  and  $\phi$  from

$$\theta = 2\pi u \quad (6)$$

$$\phi = \cos^{-1}(2v - 1). \quad (7)$$

Using the equations above we generate a position in the random catalogue. If this position is inside the boundaries of the data catalogue, then a temperature of the data catalogue is associated with that random vector. This procedure is repeated until the random catalogue has the same number of “objects” as the data catalogue. This method, also known as “bootstrapping”, involves resampling the data with replacement and, at random, to construct a new data set which has population distribution identical to that of the original dataset. Figure 1 shows a realization of one of our mock catalogues.

### C. VLSS: The VLA Low-Frequency Survey

The VLA Low-frequency Sky Survey (VLSS, formerly known as 4MASS) is a 74 MHz (or 4 meter wavelength) continuum survey carried out by the National Radio Astronomy Observatory (NRAO) and the Naval Research Laboratory (NRL). The aim of the survey is to map an area of  $3\pi$  sr covering the entire sky north of  $-30^\circ$  declination at resolution  $80''$  (FWHM), with an average noise level of 0.1 Jy/beam. The principal data product is a set of 358 continuum images of  $(14^\circ \times 14^\circ)$ , and a cata-

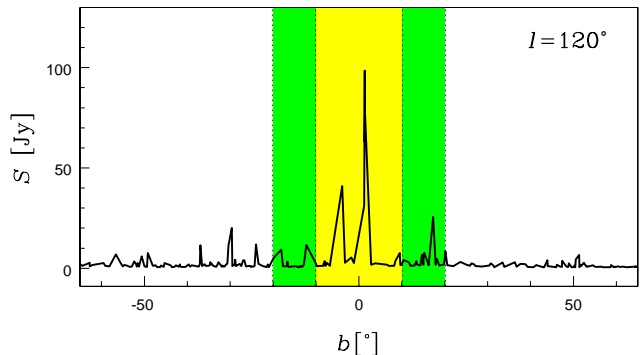


FIG. 4: The signal as a function of galactic latitude for a constant galactic longitude of  $\ell=120^\circ$ . Green and yellow shades enclose the regions  $|b| \leq 20^\circ$  and  $|b| \leq 10^\circ$ , respectively. Sources within these shaded regions are masked from our analysis as they may be galactic in origin.

logue with 68,311 discrete sources [58]. The VLSS catalogue was created by fitting elliptical Gaussians to all the sources that are detected at the 5 sigma level or higher [64], and it is complete at the 770 mJy level [65]. The 74 MHz catalogue is shown in Figure 1, top, and a comparison of this survey with other low-frequency surveys can be seen in Table II and Figure 2.

## III. RESULTS

In Figure 3, we present our measurement of  $w(\theta)$  for the flux limit of  $S = 770$  mJy (black squares), which is the completeness limit of the VLSS catalogue. Distances between data and/or random sources are measured in bins of  $0.09^\circ$ , which is safely above the VLSS resolution limit of  $0.02^\circ$ . We also investigated if  $w(\theta)$  changes with bin size, and we found no indication that any change in bin size affects our results.

As shown in Figure 4, there are sources in the VLSS catalogue that may be galactic in origin. In this figure, we plot the source fluxes at galactic longitude  $\ell=120^\circ$  as a function of galactic latitude  $b$ . The green and yellow shades enclose the regions  $|b| \leq 20^\circ$  and  $|b| \leq 10^\circ$ , respectively. To reduce contamination from galactic sources, we discarded regions inside chosen Galactic cuts; we also discarded regions below  $\delta < -10^\circ$ , due to the patch sky coverage of VLSS – see Figure 1, top.

From top-to-bottom, Figure 3 shows the measured  $w(\theta)$  for different galactic cuts. We detected no correlation for cuts smaller than  $10^\circ$  and, above this limit, there are no large variations in  $w(\theta)$ . Since we want to maximize the number of sources used in our statistics, from here on, all final calculations are for a  $10^\circ$  galactic cut (*i.e.*, for 39,118 sources). A galactic cut of  $10^\circ$  (or bigger) also excludes the “blank” regions in the VLSS survey – see Figure 1. They are regions around, *e.g.*, CasA and Cyg A.

We construct 100 mock catalogues using the procedure described in IIB, with flux values above the sensi-

TABLE IV:  $w(\theta)$ <sup>1</sup> results.

$ b $	A	$\gamma$	$w(\theta)$ □	$S_{lim}$ [mJy]	$\chi^2$
10	$0.103 \pm 0.026$	$-1.21 \pm 0.35$	0.2–0.6	770	0.62
15	$0.062 \pm 0.011$	$-1.81 \pm 0.47$	0.2–0.6	770	0.73
20	$0.041 \pm 0.007$	$-2.22 \pm 0.78$	0.2–0.6	770	0.57
25	$0.066 \pm 0.011$	$-1.81 \pm 0.28$	0.2–0.5	770	0.58
10	$0.113 \pm 0.029$	$-1.09 \pm 0.20$	0.2–0.6	850	0.86
10	$0.104 \pm 0.028$	$-1.26 \pm 0.38$	0.2–0.6	900	0.63

$S_{lim}$  = Smallest flux value.

<sup>1</sup> $w(\theta)$  is fitted by a power-law of the form  $A\theta^{-\gamma}$

tivity limit of the data catalogue and a chosen galactic cut of  $10^\circ$  applied. By cross-correlating the data with the 100 mocks, we produce a set of normally distributed estimates of the correlation function. The mean and the standard deviation of this distribution are used as a value for the estimate and its uncertainty in the measurement of  $w(\theta)$  at each  $\theta$ <sup>1</sup>. The estimate (mean) and its uncertainty (the standard deviation) are shown in Figure 3 as the black squares and their error bars. Similarly, we correlated the 100 mocks with themselves. This result correspond to the yellow shaded region shown in Figure 3 and, as expected in a Poissonian distribution,  $w(\theta)$  is consistent with zero.

We find that a single power law with shape  $w(\theta) = A\theta^{-\gamma}$  [59], where A is a measure of the amplitude of the average enhancement of the number of radio sources at a particular point in the sky, fits the data well. We present our measurements in Table IV. We also calculate  $w(\theta)$  for various flux-density limits at 770 mJy, 850 mJy and 900 mJy. As shown in Table IV and Figure 5, the amplitude of clustering does not depend on flux density. This same result was observed in previous angular correlation analysis (*e.g.*, [48]).

Some other interesting results can be taken from Figure 3: (1) at large angular separations,  $\theta \gg 2$ ,  $w(\theta)$  is consistent with zero – this is a strong evidence for a high degree of uniformity in the survey. (2) at the small angular separations,  $\theta < 0.2$ , there is a fall-off (or a break) in the value of  $w(\theta)$  – this effect is due to the failure of the survey to resolve weak double sources with separations slightly greater than the beamwidth. [66] presents a detailed explanation of this effect and show, in details, how this calculation is done. (3) Finally, at the angular separation of  $\theta \approx 1.45$ , there is an unexplained increase

<sup>1</sup> Data points in a plot of  $w(\theta)$  are not independent, *i.e.*, single sources can contribute pairs in more than one bin. Therefore, standard Poisson error bars will underestimate the true error in each bin.

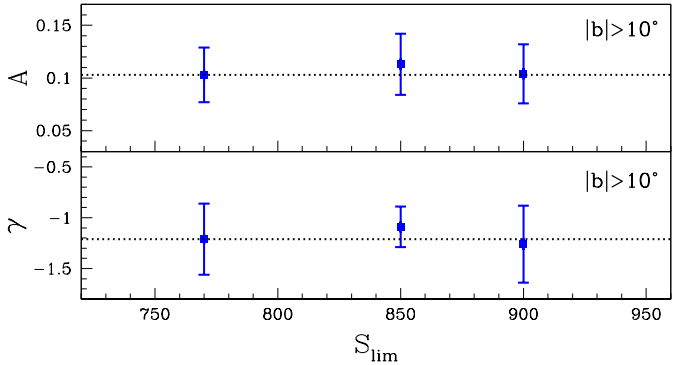


FIG. 5: Measured amplitudes of A and  $\gamma$  for various flux-density limits at 770 mJy, 850 mJy and 900 mJy. Note that the amplitude of clustering does not depend on flux density.

in the value of  $w(\theta)$ . It is well studied and reported in the literature that instrumental effects in radio surveys manifest themselves on particular characteristic scales, and are usually rendered transparent by the  $w(\theta)$  analysis (see, *e.g.*, [66]). If the anomaly described above is caused by such effects, this is something that should be carefully studied, but it is outside the scope of this paper.

#### IV. DISCUSSION

In order to construct accurate simulations at the metre wavelengths, the angular correlation of radio sources must be taken into account. The relative importance of the clustering contribution increases and may eventually become dominant if sources are identified and subtracted down to faint flux limits – which are exactly the limits involved in the point source removal of 21 cm experiments.

Using the 74 MHz VLSS survey, we measured the angular 2-point correlation function,  $w(\theta)$ . We obtain the first measurement of clustering at the low frequencies relevant to 21 cm tomography. We find that a single power law with shape  $w(\theta) = A\theta^{-\gamma}$  fits the data well. For a galactic cut of  $|b| > 10$ , with a data cut of  $\delta > -10$ , and a flux limit of  $S = 770$  mJy, we obtain a slope of  $\gamma = (-1.2 \pm 0.35)$  with  $\chi^2=0.62$ . This value of  $\gamma$  is consistent with that measured from other radio catalogues – see Table III. The amplitude of clustering has a length of 0.2–0.6, and it is independent of the flux-density threshold.

#### ACKNOWLEDGMENTS:

The authors wish to thank Joseph Lazio and Mike Matejek for helpful comments. Support for this work was provided by NSF through grants AST-0607597 and AST-0908950. JC acknowledges the Center for Excellence in Education for holding the Research Science Institute (RSI) at MIT to support this work.

- 
- [1] “The 21 cm Forest: Radio Absorption Spectra as Probes of Minihalos Before Reionization”, S Furlanetto, A Loeb 2002, *ApJ*, **579**, 1
- [2] “21 Centimeter Fluctuations from Cosmic Gas at High Redshifts”, M Zaldarriaga, S Furlanetto, L Hernquist 2004, *ApJ*, **608**, 622
- [3] “Observing the Reionization Epoch Through 21 Centimeter Radiation”, S Furlanetto, A Sokasian, L Hernquist 2004, *MNRAS*, **347**, 187
- [4] “Statistical Probes of Reionization With 21 cm Tomography”, S Furlanetto, M Zaldarriaga, L Hernquist 2004, *ApJ*, **613**, 16
- [5] “A Method for Separating the Physics from the Astrophysics of High-Redshift 21cm Fluctuations”, R Barkana, A Loeb 2005, *ApJ*, **624**, 65
- [6] “Polarization of 21cm Radiation from the Epoch of Reionization”, D Babich, A Loeb 2005, *ApJ*, **635**, 1
- [7] “Detecting the Earliest Galaxies Through Two New Sources of 21cm Fluctuations”, R Barkana, A Loeb 2005, *ApJ*, **626**, 1
- [8] “Polarization Signals of the 21 cm Background from the Era of Reionization”, A Cooray, S Furlanetto 2005, *MNRAS*, **359**, 47
- [9] “Probing the Epoch of Early Baryonic Infall Through 21cm Fluctuations”, R Barkana, A Loeb 2005, *MNRAS*, **363**, 36
- [10] “Separating out the Alcock-Paczynski Effect on 21cm Fluctuations”, R Barkana 2006, *MNRAS*, **372**, 259
- [11] “The Physics and Early History of the Intergalactic Medium”, R Barkana, A Loeb 2007, *Rep.Prog.Phys.*, **70**, 627
- [12] “Probing the Dark Ages with the Square Kilometer Array”, C Carilli, S Furlanetto, F Briggs, M Jarvis, S Rawlings, H Falcke 2004, *NewAR*, **48**, 1029
- [13] “21 cm Tomography of the High-Redshift Universe with the Square Kilometer Array”, S Furlanetto, F Briggs 2004, *NewAR*, **48**, 1039
- [14] “Observations of HI 21cm absorption by the neutral IGM during the epoch of re-ionization with the Square Kilometer Array”, C Carilli, N Gnedin, S Furlanetto, F Owen 2004, *NewAR*, **48**, 1053
- [15] “Power Spectrum Sensitivity and the Design of Epoch of Reionization Observatories”, M F Morales 2005, *ApJ*, **619**, 678
- [16] “LOFAR as a Probe of the Sources of Cosmological Reionisation”, S Zaroubi, J Silk 2005, *MNRAS*, **360**, 64
- [17] “Searching for Early Ionization with the Primeval Structure Telescope”, J Peterson, U Pen, X Wu X 2006, *IAUJD*, **12**, 18
- [18] “Multifrequency Analysis of 21 Centimeter Fluctuations from the Era of Reionization”, M G Santos, A Cooray, L Knox 2005, *ApJ*, **625**, 575
- [19] “Improving Foreground Subtraction in Statistical Observations of 21 cm Emission from the Epoch of Reionization”, M F Morales, J D Bowman, J N Hewitt 2005, *A&AS*, **207**, 3304
- [20] “21 cm Tomography with Foregrounds”, X Wang, M Tegmark, M G Santos, L Knox 2006, *ApJ*, **650**, 529
- [21] “A model of diffuse Galactic radio emission from 10 MHz to 100 GHz”, A de Oliveira-Costa, M Tegmark, B M Gaensler, J Jonas, T L Landecker, P Reich 2008, *MNRAS*, **388**, 247
- [22] “How accurately can 21 cm tomography constrain cosmology?”, Y Mao, M Tegmark, M McQuinn, M Zaldarriaga, O Zahn 2008, *PhRvD*, **78**, 3529
- [23] “Will point sources spoil 21-cm tomography?”, A Liu, M Tegmark, M Zaldarriaga 2009, *MNRAS*, **394**, 1575
- [24] “An improved method for 21-cm foreground removal” A Adrian, M Tegmark, J Bowman, J Hewitt, M Zaldarriaga 2009, astro-ph/0903.4890
- [25] “Radio and Millimeter Continuum Surveys and their Astrophysical Implications”, De Zotti, M Massardi, M Negrello, J Wall 2009, astro-ph/0908.1896
- [26] “Toward Epoch of Reionization Measurements with Wide-Field Radio Observations”, M F Morales, J N Hewitt 2004, *ApJ*, **615**, 7
- [27] “The Sensitivity of First Generation Epoch of Reionization Observatories and Their Potential for Differentiating Theoretical Power Spectra”, J D Bowman, M F Morales, J N Hewitt 2006, *ApJ*, **638**, 20
- [28] Probing the Epoch of Reionization with Redshifted 21 cm HI Emission, PhD Thesis, J D Bowman 2007, Massachusetts Institute of Technology
- [29] “Foreground Contamination in Interferometric Measurements of the Redshifted 21 cm Power Spectrum”, J D Bowman, M F Morales, J N Hewitt 2009, *ApJ*, **695**, 18
- [30] “Predictions of the Angular Power Spectrum of Clustered Extragalactic Point Sources at Cosmic Microwave Background Frequencies from Flat and All-Sky Two-dimensional Simulations”, J Gonzalez-Nuevo, L Toffolatti, F Argueso 2005, *ApJ*, **621**, 1
- [31] “A revised machine-readable source list for the Rees 38-MHz survey”, S E G Hales, E M Waldram, N Rees, P J Warner 1995, *MNRAS*, **274**, 447
- [32] “Observations of cosmic radio sources at 60 MHz”, A M Aslanyan, R D Dagkesamanskii, V N Kozhukhov, V G Malumyan, V A Sanamyan 1968, *Ap*, **4**, 39
- [33] “Radio Sources Observed with the Culgoora Circular Array (CCA) at 80 and 160 MHz”, O B Slee 1995, *AuJPh*, **48**, 143
- [34] “A radio survey of the sky north of declination 70deg at a frequency of 81.5 MHz”, N J B A Branson 1967, *MNRAS*, **135**, 149
- [35] “A sky survey at 102.5MHz: radio sources at declinations (27.5-33.5)deg and (67.5-70.5)deg”, R D Dagkesamanskii, V A Samodurov, K A Lapaev 2000, *Astron. Zh.*, **77**, 21
- [36] “Homography-based correction of positional errors in MRT survey”, V N Pandey, S Udaya 2005, URSIGA.
- [37] “The 6C Survey of radio sources”, S E G Hales, J E Baldwin, P J Warner 1988, *MNRAS*, **234**, 919
- [38] “A final non-redundant catalogue for 7C 151-MHz survey”, S E G Hales, J M Riley, E M Waldram, P J Warner, J E Baldwin 2007, *MNRAS*, **382**, 1639
- [39] “A Survey of Radio Sources at a Frequency of 159MHz”, D O Edge, J R Shakeshaft, W B McAdam, J E Baldwin, S Archer 1959, *MmRAS*, **68**, 37
- [40] “The Revised 3C Catalogue of Radio Sources”, A S Bennett 1962, *MmRAS*, **68**, 163
- [41] “A survey of radio sources between declinations 20deg and 40deg”, J D H Pilkington, P F Scott 1965, *MmRAS*,

- 69, 183
- [42] “A survey of radio sources in the declination ranges - 07deg to 20deg and 40deg to 80deg”, J F R Gower, P F Scott, D Wills 1967, *MmRAS*, **71**, 49
- [43] “Miyun 232MHz survey”, X Zhang, Y Zheng, H Chen, S Wang, S Cao, B Peng, R Nan 1997, *A&AS*, **121**, 59
- [44] “The Westerbork Northern Sky Survey”, G de Bruyn, G Miley, R Rengelink, Y Tang, M Bremer, H Rottgering, R Raimond, M Bremer, D Fullagar 2000, *yCat*, **8062**, 0
- [45] “A sample of ultra steep spectrum sources selected from the Westerbork In the Southern Hemisphere (WISH) survey”, C De Breuck, Y Tang, A G de Bruyn, H Rottgering, W van Breugel 2002, *A&A*, **394**, 59
- [46] “Texas Survey of radio sources at 365MHz”, J N Douglas, F N Bash, F A Bozyan, G W Torrence, C Wolfe 1996, *AJ*, **111**, 1945
- [47] “Clustering of 4C radio sources”, M Seldner, P J E Peebles 1981, *MNRAS*, **194**, 251
- [48] “Angular clustering in the Sydney University Molonglo Sky Survey”, C Blake, T Mauch, E M Sadler 2004, *MNRAS*, **347**, 787
- [49] “The clustering of radio sources. III - The Parkes 2700-MHz and Bologna B2 surveys”, A Webster 1977, *MNRAS*, **179**, 511
- [50] “The clustering of radio sources. IV - The 5C 5, 5C 6 and 5C 7 surveys”, A Webster 1977, *MNRAS*, **179**, 517
- [51] “The Angular Two-Point Correlation Function for the FIRST Radio Survey”, C M Cress, D J Helfand, R H Becker, M D Gregg, R L White 1996, *ApJ*, **473**, 7
- [52] “Constraints on the clustering, biasing and redshift distribution of radio sources”, M Magliocchetti, S J Maddox, O Lahav, J V Wall 1999, *MNRAS*, **306**, 943
- [53] “The spatial clustering of radio sources in NVSS and FIRST: implications for galaxy clustering evolution”, R A Overzier, H J A Rottgering, R B Rengelink, R J Wilman 2003, *A&A*, **405**, 53
- [54] “Quantifying angular clustering in wide-area radio surveys”, C Blake, J Wall 2002, *MNRAS*, **337**, 993
- [55] “Spatial Clustering of Radio Sources in the 1987 Green Banks Survey”, H Sicotte, P J E Peebles 1995, *AIPC*, **336**, 390
- [56] “Two-Point Angular Correlation Function for the Green Bank 4.85 GHz Sky Survey”, B L Kooiman, J O Burns, A A Klypin 1995, *ApJ*, **448**, 500
- [57] “The correlation function of radio sources”, A J Loan, J V Wall, O Lahav 1997, *MNRAS*, **286**, 994
- [58] “The VLA Low-frequency Sky Survey at 74MHz”, A S Cohen, W M Lane, W D Cotton, N E Kassim, T J W Lazio, R A Perley, J J Condon, W C Erickson 2006, *yCat*, **8079**, 0
- [59] “The Large Scale Structure of the Universe”, P J Peebles 1980, Princeton University Press
- [60] “Bias and variance of angular correlation functions”, S D Landy, A S Szalay 1993, *ApJ*, **412**, 64
- [61] “Toward Better Ways to Measure the Galaxy Correlation Function”, A J S Hamilton 1993, *ApJ*, **417**, 19
- [62] <http://mathworld.wolfram.com/SpherePointPicking.html>
- [63] “CRC Concise Encyclopedia of Mathematics”, E W Weisstein 2002, Chapman & Hall/CRC Press, 2nd edition, 3242p.
- [64] “Detecting Radio Sources with Machine Learning”, K E McGowan, W Junor, T J W Lazio 2005, *ASPC*, **345**, 362
- [65] “The Low-Frequency Radio Counterpart of the XMM Large-Scale Structure Survey”, A S Cohen, H J A Rottgering, N E Kassim, W D Cotton, R A Perley, R Wilman, P Best, M Pierre, M Birkinshaw, M Bremer, A Zanichelli 2003, *ApJ*, **591**, 640
- [66] “Measurement of the angular correlation function of radio galaxies from the NRAO VLA sky survey”, C Blake, J Wall 2002, *MNRAS*, **329**, L37